molecular pharmaceutics

Article

pubs.acs.org/molecularpharmaceutics

Chitosan Microparticles and Nanoparticles as Biocompatible Delivery Vehicles for Peptide and Protein-Based Immunocontraceptive Vaccines

Brendon Y. Chua,[†] Mohammad Al Kobaisi,[‡] Weiguang Zeng,[†] David Mainwaring,[‡] and David C. Jackson*[,†]

[†]Department of Microbiology and Immunology, The University of Melbourne, Royal Parade, Parkville, Australia 3010

[‡]School of Applied Sciences, Royal Melbourne Institute of Technology, Melbourne, Australia 3010

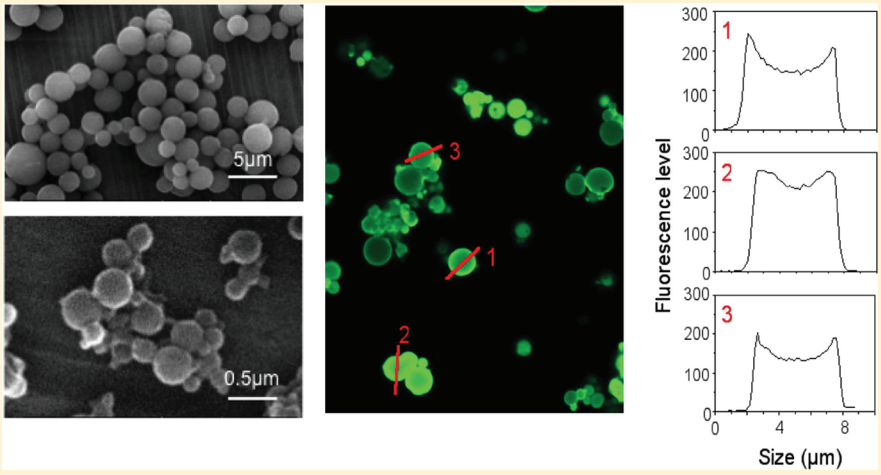

ABSTRACT: It has become increasingly recognized that polymer particle size can have a profound effect on the interactions of particle-based vaccines with antigen presenting cells (APCs) thereby influencing and modulating ensuing immune responses. With the aim of developing chitosan particle-based immunocontraceptive vaccines, we have compared the use of chitosan-based nanoparticles and chitosan-based microparticles as vaccine delivery vehicles for vaccine candidates based on luteinizing hormone-releasing hormone (LHRH). Particles, functionalized with chloroacetyl groups, which allows the covalent attachment of thiol-containing antigens, were able to adsorb ~60−70% of their weight of peptide-based antigen and 10−20% of their weight of protein-based antigen. Quantitation by amino acid analysis of antigen associated with particles demonstrated a correlation between associated antigen and the degree of chloracetylation of particles. Visualization of fluorescently labeled antigen-loaded particles by confocal microscopy indicated that the majority of antigen was localized at the particle surface with a smaller amount located in the interior. We also found that uptake of both fluoresceinated nanoparticles and microparticles by dendritic cells occurred in a manner dependent on particle concentration. Nanoparticles trafficked from the injection site to draining lymph nodes faster than microparticles; high numbers of nanoparticle-bearing cells appeared in draining lymph nodes on day 3 and microparticles on day 4. This difference in trafficking rate did not, however, appear to have any significant impact on the ensuing immune response because inoculation with both peptide-conjugated and protein-conjugated particles induced high levels of LHRH-specific antibodies. In the case of protein-conjugated particles, the levels of antibodies elicited were similar to those elicited following inoculation with antigen emulsified with complete Freund's adjuvant. The approach to vaccine design that we have described here could represent another useful method for inducing immune responses against microbial, viral and tumorigenic protein antigens.

KEYWORDS: *nanoparticles, microparticles, chitosan, immunocontraception, vaccine delivery*

INTRODUCTION

Chitosan is a nontoxic linear polysaccharide composed of β-1,4-linked D-glucosamine derived from the deacetylation of chitin, a naturally occurring polymer found in the exoskeletons of crustaceans and insects. Because of its biocompatibility and biodegradability into nontoxic and nonallergenic products, chitosan is commonly used for many applications in pharmaceutical and medical fields. Many studies on various forms of chitosan, including chitosans with varying degrees of

Received: May 20, 2011
Revised: September 28, 2011
Accepted: December 7, 2011
Published: December 7, 2011

dx.doi.org/10.1021/mp200264m | *Mol. Pharmaceutics* 2012, 9, 81−90

acetylation and chemically modified chitosans, have investigated their ability to act as vaccine delivery systems.[1] The uses of both solution and particulate forms of chitosan to increase the efficacy and response to immunization with model protein antigens,[2−4] DNA plasmids,[5,6] viral antigens,[7−9] bacterial derived toxins[10−12] and antigens[13,14] are well documented.

Although the mechanisms mediating the adjuvanticity of these derivatives are yet to be fully explained, it has become increasingly apparent that polymer particle dispersity in terms of size and shape distributions can have a profound effect on particles and their interactions with antigen presenting cells (APCs) and may hence influence the magnitude of the ensuing immune responses. Fifis et al.[15] have demonstrated that an optimum particle size for inducing both cell- and antibody-mediated responses with polystyrene beads loaded with antigen is 40−50 nm. Nanoparticles in this size range have also been found to preferentially induce Th1-biased responses while larger particles are conducive at mediating a Th2-type response.[16] These observations may be explained by reports that smaller particles appear to be trafficked faster and by different dendritic cell subsets from the injection site to the draining lymph nodes compared to their larger counterparts.[17,18] Furthermore, particles of this size are better able to stimulate proinflammatory cytokine secretion.[19] In contrast to these studies, however, Cohen et al.[20] have also shown that polyacrylamide particles in nano- or micrometer diameter size ranges are equally effective at stimulating T cell proliferation and cell-mediated responses. Furthermore, microparticles in the size range 500−3000 nm but not smaller demonstrate higher efficiencies for cross-presentation of antigen by dendritic cells.[21] No differences in macrophage responses were observed upon exposure to different sized particles.[22]

Although these differences in findings could be due to the different materials used, the results do emphasize the impact that particle size can have in shaping the ensuing immune responses and that selection of an optimum particle size is an important consideration in the development of a particulate vaccine delivery system.

With the aim of developing chitosan particle-based vaccines, we have compared the use of chitosan-based nano- and microparticles as vaccine carriers for peptide and protein antigens based on luteinizing hormone-releasing hormone (LHRH). LHRH is a 10 amino acid peptide hormone that is secreted by the hypothalamus and initiates a cascade of events that regulates gametogenesis.[23] Antibodies generated against this hormone can lead to the inhibition of reproductive capabilities of vaccinated animals.[24−27] Because its sequence is conserved in all mammals, the use of an immunocontraceptive vaccine based on LHRH has potential as an alternative to surgical castration in companion animals and livestock[28] and even for the control of hormone dependent malignancies in humans.[27,29] Nano- and microparticles, produced by varying the type of surfactant in the synthesis process, were functionalized with chloroacetyl groups to allow for the covalent attachment of thiol-containing peptide and protein antigens. The antigen loading capacities of the particles were investigated qualitatively by flow cytometry and confocal microscopy and quantitatively by amino acid analysis. Nano- and microparticles loaded with antigen were then examined for their ability to be taken up by dendritic cells, to traffic to draining lymph nodes and to induce anti-LHRH antibodies in mice.

MATERIALS AND METHODS

Synthesis of Chitosan-Based Particles. Low molecular weight chitosan having M_n of 164 kDa, 75−85% degree of deacetylation and a viscosity of 0.026 Pa·s for a 1 wt % solution in 1% acetic acid, and glutaraldehyde (50 wt % solution in water), and Tween 80 and Span 80 were obtained from Sigma-Aldrich. Sodium borohydride (98%) was from Sigma, chloroacetic anhydride (95%) was from Aldrich and chloroacetic acid (99%) was obtained from Sigma-Aldrich. Paraffin oil having a viscosity of 0.130 Pa·s was obtained from Chem-Supply Pty. Ltd. Emulsions were prepared with a high shear mixer (Ultra Turrax, Germany) using an 18 mm stator diameter (S25N-18G). Typical emulsions were prepared by dissolving predetermined amounts of surfactant in 250 mL of paraffin oil followed by addition of 25 mL of 1.5% chitosan in water containing 1% acetic acid and 0.9% NaCl over a period of 10 min (Table 1). Immediately, 15 mL of glutaraldehyde saturated

Table 1. The Weight Fractions of Tween 80 and Span 80 Surfactants Used To Produce Chitosan Particles with Different Size Distribution

X_{T80}	X_{S80}	HLB	V_{surf}[a] (mL)	part. type	part. size distribn
	1.00	4.3	2.2	nano	30−500 nm
0.37	0.63	8.2	1.4	micro	1−6 μm

[a] V_{surf} is the surfactant volume used in 250:25 o/w emulsion.

toluene (GST) was added dropwise to the emulsion with continuous stirring at 500 rpm using a mechanical stirrer. The cross-linking reaction was allowed to proceed for 3 h with stirring. Cross-linked particle suspensions were then centrifuged at 1268g−14087g depending on the particle size distribution required. The resulting particles were resuspended in a hexane/acetone mixture and recentrifuged. This was repeated with acetone and finally water washed several times to remove residual paraffin oil, surfactants, sodium chloride and other excipient reagents.

ImageJ 1.42q software (National Institutes of Health, USA) was used to obtain particle diameters for the statistical size analysis of the SEM images of the various chitosan particles. PeakFit (Version 4.12, Seasolve) was used to fit a function to the particle size distribution obtained by ImageJ software. Populations were counted in 10 nm brackets for the nanoparticles and 0.5 μm brackets for the microparticles, and the total number counted per sample was ∼1,000 particles. The size distribution was fitted to a log-normal amplitude function.

The particles were reduced in 1% w/w $NaBH_4$ in methanol. The reduction process was repeated twice for 30 min followed by washes using methanol, acetone/water and then acetone. Chloroacetylation of particles was carried out by incubating reduced particles in a solution containing 0.3 g of chloroacetic anhydride and 1 g of chloroacetic acid in 25 mL of acetone at 50−60 °C for 1 h. The particles were then washed thoroughly with acetone and water to remove nonreactive species and then freeze-dried.

To quantify the number of chloroacetyl groups available for reaction with thiol groups, particles (1.5 mg/mL) were incubated with 40 nM 2-mercaptoethanol for 2 h at 37 °C in 0.1 M phosphate buffer (pH 8.3). 100 μL of supernatant was removed and 50 μL of 10 mM 5,5′-dithiobis(2-nitrobenzoic acid) (DTNB) added and incubated at room temperature for 15 min. The absorbance of this solution was then measured at

dx.doi.org/10.1021/mp200264m | Mol. Pharmaceutics 2012, 9, 81−90

412 nm and the amount of thiolate present as a result of reaction with 2-mercaptoethanol determined using a molar extinction coefficient of 13,700 M^{-1} cm^{-1} for DTNB.

Scanning electron microscopy (SEM) examination of particle preparations was carried out using a Philips XL30 (USA) scanning electron microscope. Samples were prepared by dispersing chitosan particles onto an adhesive carbon tape fixed to the aluminum sample holder and sputter coated with gold using a SPI-Module Sputter Coater (West Chester, PA, USA).

For some experiments, empty particles were fluoresceinated by incubation of a 1 mL suspension of particles (30 mg/mL) with 1 mL of a solution (5 mg/mL) fluorescein isothiocyanate (FITC) at 37 °C in 0.1 M phosphate buffer (pH 8.3) for 24 h. Fluoresceinated particles were washed extensively 10 times with 0.1 M phosphate buffer and then 5 times with dimethyl sulfoxide to solubilize any insoluble FITC that may have precipitated during the incubation period. Final washes were performed with water (5−7 times) until the supernatants from preparations containing fluoresceinated particles remained clear for more than 4 h. Particles were then freeze-dried (Labconco Freezone 4.5 freeze-drying system, USA) until used.

Vaccine Antigens. The peptide antigen used was composed of the sequence ALNNRFQIKGVELKS, which is derived from the influenza virus hemagglutinin light chain of the H3 subtype and is recognized by I-E^d restricted $CD4^+$ T helper cells.[30] This epitope was assembled in a collinear fashion with the LHRH peptide sequence HWSYGLRPG using conventional solid-phase methodologies as described elsewhere.[31] In some cases, a cysteine residue was inserted at the N-terminus of the peptide to enable subsequent covalent attachment of peptide to chloroacetylated particles using thioether chemistry and peptide was sometimes fluoresceinated using 5(6)-carboxyfluorescein (Fluka BioChemika, Switzerland) as described previously.[32]

The protein antigen used was a proprietary protein-based vaccine (Improvac, Pfizer Australia). This vaccine is composed of the synthetic peptide LHRH covalently conjugated to a carrier protein. Free thiol groups were quantitated using DTNB [5,5′-dithiobis(2-nitrobenzoic acid)]. Fluorescent labeling of protein was carried out as previously described[32] and fluoresceinated protein purified by gel permeation chromatography using a Superdex 75 10/300 GL column (Amersham Biosciences, Sweden) installed in an AKTA FPLC system.

Loading and Quantification of Antigen Uptake by Chitosan Particles. In order to determine the amount of the antigen that could be passively absorbed by particles i.e. the efficiency of loading, 1 mL of a solution containing either peptide or protein (2.5 mg/mL) in 0.1 M phosphate buffer (pH 8.3) was added to dried particles. In this way 2.5 mg of antigen was added to 2.5 mg of dry particles in a total volume of 1 mL and the preparation immediately centrifuged at 900*g* for 5 min. An aliquot of the supernatant was then taken to determine the starting amount of antigen present. This was done by measuring the optical density of the supernatant (214 nm for peptide and 280 nm for protein). The preparation of sedimented particles was resuspended in the same supernatant and incubated at 37 °C on a mixing rack. The amount of antigen uptake was determined after 24 h by determining the amount of antigen remaining in the supernatant after 24 h.

The amount of antigen covalently attached to particles using thioether chemistry was determined following extensive washing to remove unbound antigen. Each wash step consisted of centrifugation and resuspension of particles in double distilled water. The particles were allowed to stand for 10 min in water between washes and were freeze-dried after the last wash. Particles were reconstituted in water at 1 mg/mL concentration and 100−300 μg aliquots dried in 300 μL sample vials (Waters, USA) by vacuum centrifugation. Microwave (Discovery Research System, CEM Corporation, USA) vapor-phase hydrolysis of particles was then performed using 6 N HCI containing 0.1% phenol. Hydrolyzed samples were derivatized with Waters AccQTag reagents according to the manufacturer's instructions, and amino acid analysis was conducted on a Waters Acquity UPLC System using an AccQTag ultra column (2.1 × 100 mm).

Confocal Microscopy and Flow Cytometric Analysis of Fluoresceinated Antigen-Conjugated Chitosan Particles. Further evaluation of antigen conjugation was verified by conjugating fluoresceinated antigen to particles. After extensive washing, particle fluorescence was analyzed on a FACSCalibur flow cytometer (Becton Dickinson, USA). Fluoresceinated antigen-conjugated particles were also examined using a confocal scanning laser system (Ziess LSM-510 Meta) installed on a Zeiss Axioplan2 microscope. Fluorescence was visualized using a 488 nm excitation filter and a 522/535 nm emission filter for fluorescein. The same pinhole and photomultiplier gain and laser power level settings were used for all samples examined. Single 1024 × 1024 pixel images (0.5 mm optical section) were captured using a 63× objective lens. Fluorescence intensity cross-section profiles were determined using Image J software.

Dendritic Cell Particle Uptake and *in Vivo* Trafficking of Particles. To determine cell uptake of particles *in vitro*, bone marrow-derived dendritic cells (DCs) were generated. Briefly, the femurs and tibias of BALB/c mice were removed and the bone marrow was flushed out with PBS. The bone marrow suspension was washed and then cultured at a concentration of 2 × 10^6 cells in 10 mL of RPMI-1640 (Invitrogen, USA) supplemented with 10% heat inactivated FCS (CSL, Parkville, Australia), gentamicin (12 mg/mL), 2 mM glutamine, 1 mM sodium pyruvate, penicillin (100 IU/mL), streptomycin (100 μg/mL), 55 μM 2-mercaptoethanol and 200 U/mL of recombinant GM-CSF (BioLegend, Australia) in 100 mm diameter bacterial Petri dishes (Becton Dickinson, Germany). Fresh medium (10 mL) was added on day 3, and half medium changes were performed on days 6 and 8. On day 10, nonadherent and slightly adherent cells were collected and incubated (5 × 10^5 cells/mL) with varying amounts of fluoresceinated particles in a 24-well plate (Nunc, Denmark). After 24 h, cells were collected in a 10 mL tube. Any free or non-cell associated particles were removed by gently underlaying each suspension with 2 mL of Ficoll Paque (Amersham Pharmacia, Sweden). Samples were then centrifuged at 910*g* for 20 min with the centrifuge brake off. Cells were collected at the Ficoll Paque−medium interface leaving free particles sedimented at the bottom of the tube. These were then washed extensively with FACs Wash (PBS supplemented with 5 mM EDTA and 5% FCS). Cell surface-associated fluorescence was quenched by incubating cells with an equal volume of 0.1 M citrate buffer pH 4 containing 250 μg/mL of trypan blue and intracellular fluorescence associated with fluoresceinated particle uptake then analyzed by flow cytometry. Data analysis was performed using FlowJo software (Treestar Inc., USA). Viable cells were gated based on their forward and side scattering properties and analysis were performed on total of 1 × 10^4 cells.

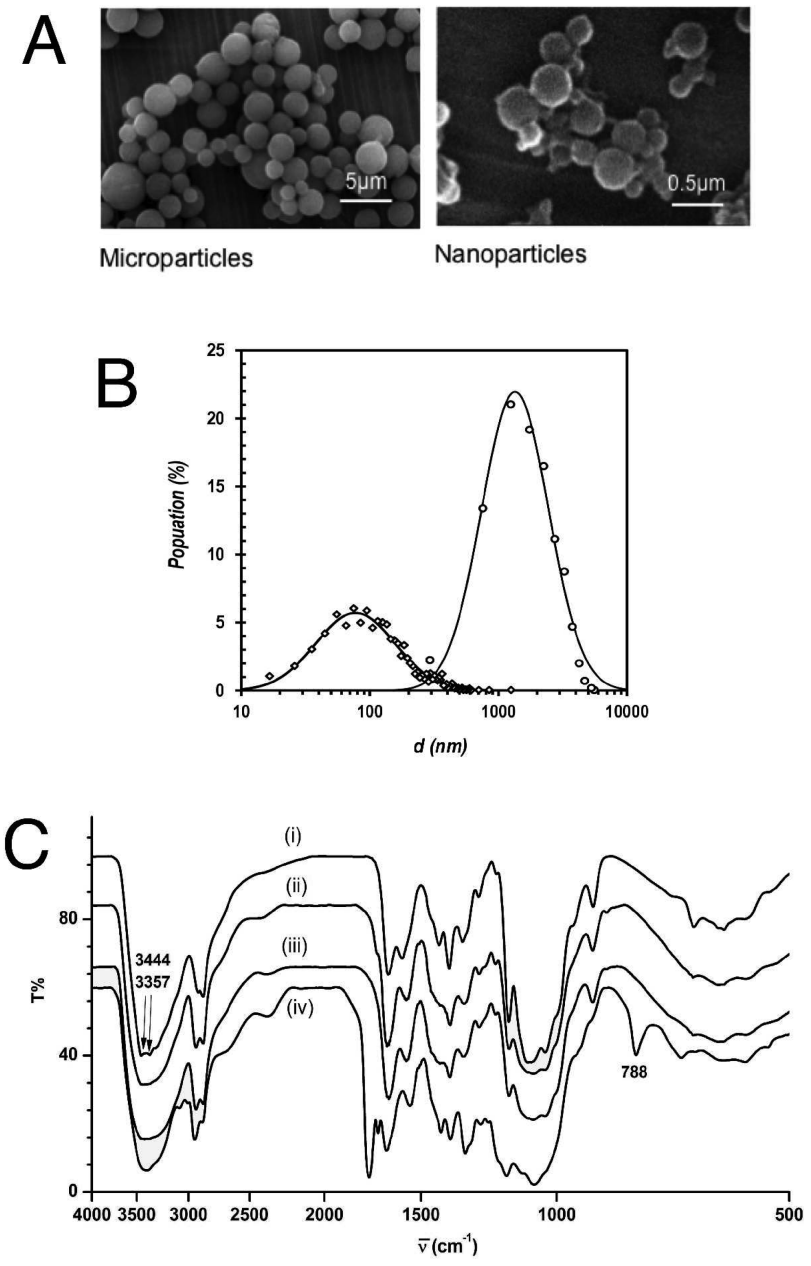

Figure 1. A) Scanning Electron Micrographs of different sized chitosan-based particles. B) The size distribution of chitosan micro and nanoparticles showing the diameter (d) in nanometers (nm), C) FTIR spectra of i) chitosan, ii) glutaldehyde cross-linked chitosan particles, iii) reduced cross-linked chitosan particles and iv) chloroacetylated chitosan particles.

To detect trafficking of particles *in vivo*, groups of female 8–10 week old BALB/c mice were inoculated in the footpad with 200 μg of fluoresceinated micro- or nanoparticles in a volume of 50 μL of normal saline. For each time point examined, 2 mice from each group were killed and popliteal lymph nodes removed. Single cell suspensions were obtained by passing lymph nodes through a 50 μm cell sieve (Becton Dickinson, USA). Cells were then incubated in RPMI-1640 supplemented with 1 mg/mL collagenase (Roche, Germany) and 0.1% w/v DNase (Boehringer, Germany) for 30 min at 37 °C and washed with FACs Wash prior to flow cytometric analysis.

Enzyme-Linked Immunosorbent Assays. All experimental procedures involving animals have been approved by the University of Melbourne's animal ethics committee (0808667). To determine the magnitude of antibody responses following vaccination with antigen-loaded particles, groups of five female 8–12 week old BALB/c mice were inoculated subcutaneously in the base of the tail on day 0 and again on day 22 with amounts of particles containing the equivalent of 25 μg of protein or 20 nmol of peptide antigen. Controls included groups of animals that received protein or peptide antigen administered in saline or emulsified with Complete Freund's Adjuvant (CFA; Sigma Aldrich, St. Louis, USA). Sera were prepared from blood taken at 3 weeks following the primary inoculation and 2 weeks following the secondary inoculation.

Flat bottom well polyvinyl plates were coated with LHRH peptide (5 μg/mL) in phosphate buffered saline (PBS) for 18–20 h at room temperature in a humidified atmosphere. The antigen was removed and BSA (10 mg/mL) in PBS added for 1 h before washing with PBST (PBS containing v/v 0.05%

dx.doi.org/10.1021/mp200264m | *Mol. Pharmaceutics* 2012, 9, 81–90

Table 2. Total Amount of Antigen Taken Up by Particles

particle type	amt of peptide[a] (μg)	loading effic[b] (%)	amt of protein[a] (μg)	loading effic[b] (%)
microparticles	617 ± 112.6	24.7 ± 4.5	263.1 ± 29.1	10.4 ± 1.1
nanoparticles	734.1 ± 38.4	29.4 ± 1.5	105.3 ± 31.7	4.2 ± 1.2

[a]Expressed as amount per mg of particles. [b]Expressed as a percentage of the starting amount of peptide or protein used.

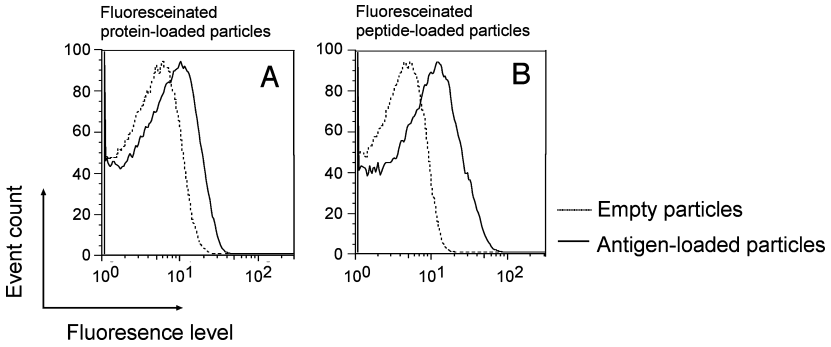

Figure 2. Flow cytometric analysis of antigen-conjugated microparticles. Microparticles (2.5 mg/mL) were mixed with either fluoresceinated protein (A) or fluoresceinated peptide (B) antigens at a concentration of 5 mg/mL in 0.1 M phosphate buffer (pH 8.3) for 24 hours at 37 °C. Particles were washed extensively and then analyzed by flow cytometry. The fluorescence profiles of antigen-loaded particles (solid line) are shown and compared to nonloaded particles (broken line).

Tween-20 [Aldrich, Milwaukee, USA]). Serial dilutions of sera obtained from immunized mice were added to wells and incubated overnight at room temperature in order to detect anti-LHRH antibodies. After washing with PBST, bound anti-LHRH antibody was detected using horseradish peroxidase-conjugated rabbit anti-mouse IgG antibodies (Dako, Glostrup, Denmark) in conjunction with enzyme substrate (0.2 mM 2,2′-azino-bis(3-ethylbenzthiazoline-sulfonic acid) in 50 mM citric acid containing 0.004% hydrogen peroxide). The titers of anti-LHRH antibody are expressed as the reciprocal of the highest dilution of serum required to achieve an optical density of 0.2.

Statistical Analyses. All statistical analysis was carried out using one-way ANOVA nonparametric statistical analysis using Prism 4 (GraphPad software Inc., USA). Tukey's multiple comparison tests were used to analyze data sets between all groups.

RESULTS

Synthesis of Chitosan-Based Particles. To produce chitosan-based particles for this study, a high-sheer emulsification process was employed. Varying the hydrophilic/lipophilic balance (HLB) of the surfactant used in this technique allowed for greater control over particle size distribution. Table 1 lists the mixing ratios of the surfactants used to obtain the necessary HLB values, and scanning electron microscopy images in Figure 1A show distinct size ranges for the resulting chitosan particles. Figure 1B shows that a high HLB value (8.2) produced particles with a centroid of 2.10 μm such that 92% of the microparticles were in the range 1.62−2.58 μm while the lower HLB value (4.3) produces nanoparticles with a centriod of 163 nm 92% in the range 113−213 nm. For the covalent attachment of macromolecular cargo to these particles, a chloroacetylation strategy was adopted.[33] Incorporation of chloroacetyl groups provides functional sites to tether protein or peptide cargo containing free thiol groups such as those found in cysteine residues. FTIR spectroscopy was used to confirm the chloroacetylation process. The peak at ~788 cm^{-1} (assigned to C−Cl stretching) confirmed the presence of the chloroacetyl functionality; no amine functionality is available in the cross-linked particles; this is apparent from the disappearance of the N−H symmetric and asymmetric stretching peaks at 3444 and 3357 cm^{-1} peaks (Figure 1C). The substitution factor of each particle type was subsequently confirmed by measuring the binding of 2ME. All particle types examined were found to contain varying amounts of chloroacetyl groups (Table 2) with nanoparticles containing more chloroacetyl groups than microparticles.

Location and Quantitation of Antigen Cargo Present in Chitosan Particles. The ability of synthesized particles to take up peptide or protein cargo was determined by incubation with a 3 kDa immunocontraceptive peptide-based vaccine candidate[34] or a 68 kDa proprietary protein-conjugate vaccine. In the case of the peptide vaccine, a cysteine residue was inserted at the N-terminus so that covalent binding to chloroacetyl groups on the particles could be achieved through the formation of thioether bonds at this position. For the protein, the presence of free thiol groups was first determined by DTNB binding which indicated that each gram of purified protein contained 21.06 ± 0.92 nmol of thiol groups available for binding (data not shown).

Each of the vaccines was incubated with the different particle types in phosphate buffered solutions at pH 8.3 and 37 °C to provide optimal conditions for both covalent binding and noncovalent adsorption of vaccines to the particles. Spectrophotometric measurements were then taken at various time points to determine the amount of peptide or protein remaining in solution. Each particle type was found to absorb approximately 60−70% of its weight in peptide antigen and 10−20% of its weight in protein antigen over an incubation period of 24 h (Table 2). No significant differences in the amount of vaccine taken up by either particle type were detected.

To confirm the presence of peptide or protein cargo associated with particles, the fluorescence of microparticles incubated with fluoresceinated peptide or protein was measured by flow cytometry (Figure 2). Particles incubated with either fluoresceinated peptide or fluoresceinated protein displayed higher fluorescence than nonloaded particles confirming

dx.doi.org/10.1021/mp200264m | Mol. Pharmaceutics 2012, 9, 81−90

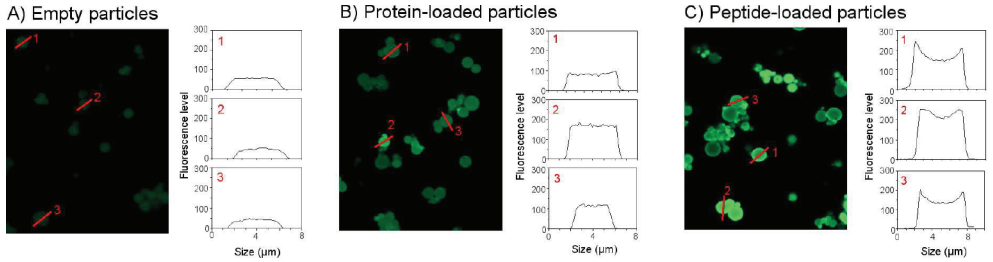

Figure 3. Confocal microscopic analysis of microparticles to which antigen has been covalently attached. The fluorescence intensity of unloaded (A), protein loaded (B) or peptide loaded (C) microparticles was obtained across the width of individual particles using a confocal scanning laser microscope system. Fluorescence was visualized using a 488 nm excitation filter and a 522/535 nm emission filter for fluorescein. The same pinhole and photomultiplier gain and laser power level settings were used for all samples examined. Images were captured using a 63× objective lens. The fluorescence profile from each numbered particle cross section (red line) is shown on the left of each microscopic image.

uptake. In agreement with spectrophotometric measurements, greater fluorescence intensities were associated with particles incubated with fluoresceinated peptide compared to those incubated with fluoresceinated protein.

The fluorescence intensity profiles of cross sections of representative particles were also derived using confocal microscopy to determine the localization of fluoresceinated antigen. Fluorescence intensities observed in cross sections of microparticles that were treated with fluoresceinated protein were evenly distributed over the particle surface and throughout the interior (Figure 3A,B). In those particles that were treated with fluoresceinated peptide, slightly higher fluorescence intensities were located at the surface than within the interior of the particle (Figure 3C).

Visual examination and fluorescence analysis of nanoparticles by confocal microscopy and flow cytometry could not be performed because the size of these particles falls below the minimum sample size detection limits for both techniques.

In order to accurately quantitate the amount of antigen that was covalently attached to particles, loaded particles were washed extensively and amino acid analysis then performed to quantitate the amount of associated protein. It was found that the amount of antigen detected was inversely proportional to particle size with significantly larger amounts of peptide or protein associated on nanoparticles than on microparticles. This correlates with the number of chloroacetyl groups present on these particles (Table 3). Therefore although there were very little differences in the amount of cargo that can be absorbed by these particles, it appears that particle size may be an influential factor for the amount of antigen that can be covalently conjugated.

Table 3. Amount of Chloroacetyl Groups Associated with Particles

particle type	amt of $ClCH_2CO$ groups (nmol)[a]	amt of conjugated peptide (μg)[a]	amt of conjugated protein (μg)[a]
microparticles	241.6	17.2 ± 5.9	14.3 ± 3.46
nanoparticles	485.0	25.3 ± 2.9	58.6 ± 6.1

[a]Expressed as amount per mg of particles.

Dendritic Cell Particle Uptake and *in Vivo* Trafficking of Particles. A key requirement for the generation of immune responses is the internalization of antigen by dendritic cells (DCs). Antigens are then processed by degradative proteolytic mechanisms for subsequent presentation on surface MHC molecules where they can be recognized by specific T cells.

In order to determine if particles can be internalized by DCs, non-antigen loaded particles were fluoresceinated and uptake by murine bone marrow-derived DCs was assessed *in vitro*. To ensure that antigen cargo would not influence the cellular uptake of particles, non-antigen loaded particles were used as a control. Intracellular-associated fluorescence was measured following washing to remove any free particles in culture, and extracellular fluorescence was quenched by the addition of trypan blue.

The results of the experiment (Figure 4A) demonstrate that uptake of both fluoresceinated nanoparticles and fluoresceinated microparticles by DCs occurred in a concentration-dependent manner. The presence of 6 μg of particles in culture was sufficient to facilitate uptake by 25% of DCs, and up to approximately 75% of DCs were found to have internalized particles when a 50 μg dose of microparticles was used. At all concentrations examined, both nanoparticles and microparticles show similar abilities to be taken up by dendritic cells. The intracellular localization of particles was also confirmed by confocal microscopy which demonstrated the presence of fluorescent spherical bodies distributed within the cell interior (Figure 4B).

In order for DCs to present processed antigen to T cells, the DC must traffic to the draining lymph nodes where naive T cells reside. To investigate whether uptake of particles by cells *in vivo* resulted in their transport to lymph nodes, mice were vaccinated in the footpad with fluoresceinated nano- or microparticles followed by examination of the popliteal lymph nodes for the presence of fluorescence positive cells.

No particle-associated cells could be detected in lymph nodes during the first two days following inoculation (Figure 5). On day 3, however, populations of cells containing either nanoparticles or microparticles could be detected in the lymph node with significantly more fluorescence positive cells observed following inoculation with nanoparticles than with microparticles. Phenotypic analysis of lymph node cells using antibodies against cell lineage markers (data not shown) revealed that both nanoparticles and microparticles were associated with dendritic cells (for nanoparticles, $CD11c^+$ cells = 43.5% ± 24.5; for microparticles, $CD11c^+$ cells = 30.5% ± 2.3) and macrophages (for nanoparticles, $F4/80^+$ cells = 47.5% ± 2.1; for microparticles, $F4/80^+$ cells = 46.5% ± 12.0).

Nanoparticle trafficking to the spleen reached a maximum on day 3 and declined thereafter although there was a trend for higher than background levels on day 7. Microparticle trafficking reached a maximum on day 4 and had dropped by

dx.doi.org/10.1021/mp200264m | *Mol. Pharmaceutics* 2012, 9, 81–90

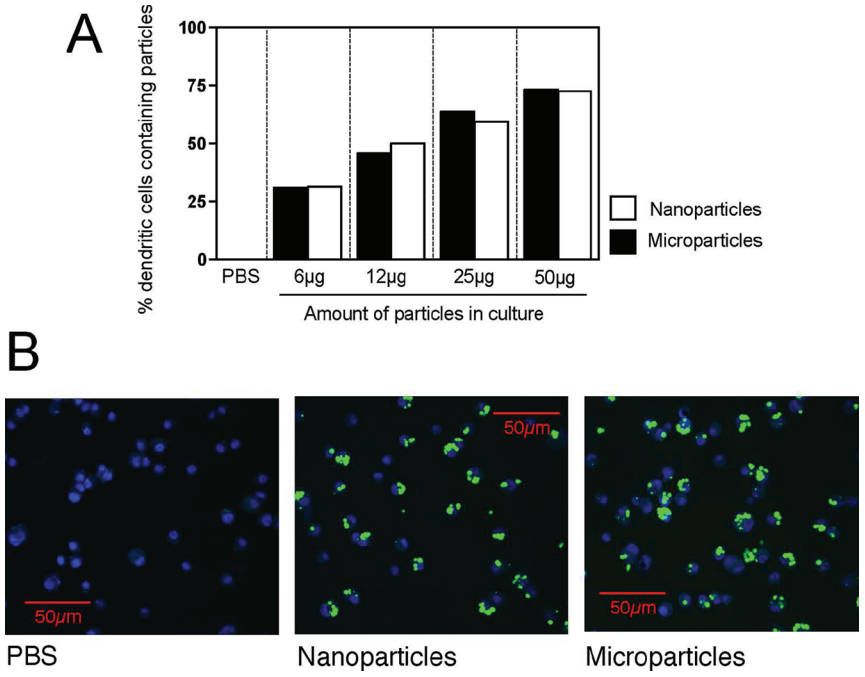

Figure 4. Uptake of fluoresceinated nanoparticles and microparticles by dendritic cells. Bone marrow-derived dendritic cells (5×10^5 cells/mL) were incubated with varying amounts of fluoresceinated microparticles or nanoparticles for 24 h at 37 °C. Particles that were not associated with cells were removed by Ficoll Paque gradient separation, and extracellular fluorescence was quenched using the dye trypan blue. (A) Cells were analyzed by flow cytometry to determine the level of intracellular fluorescence associated with particle uptake. A minimum of 1.5×10^4 viable cells with similar size and granularity in the forward and side-scatter plots were analyzed. Cell-associated autofluorescence was eliminated from analysis by visualizing fluorescence dot plots on the FL1 vs FL2 channels. The amount of fluorescent particle positive cells in each sample was determined using a quadrant marker that was set such that <0.05% of untreated cells were included. (B) Confocal micrographs of cells which have taken up fluoresceinated particles were obtained using identical photomultiplier gain and laser power levels set to eliminate background fluorescence. The images shown were derived at the cell midheight.

day 7, but again there was a trend for higher than background fluorescence at this time.

Immunogenicity of Antigen-Conjugated Particles. To evaluate the immunogenicity of vaccine-loaded particles, mice were inoculated with two doses of nanoparticles or microparticles that had been loaded with similar amounts of protein or peptide antigen. The levels of LHRH-specific antibody responses in these animals were subsequently determined and compared with those in animals that had received the same amount of antigen delivered in saline or emulsified in complete Freund's adjuvant (CFA).

In the case of the protein-based vaccine (Figure 6A), very high antibody titers were elicited when the vaccine was administered with Freund's complete adjuvant; this was true in both the primary and secondary responses. High titers of antibody were also induced by antigen-loaded nanoparticles and microparticles, but two doses were necessary to reach the levels that were achieved with Freund's complete adjuvant. The protein-based vaccine when administered in saline elicited very little if any antibody after a single dose of vaccine and levels of antibody that were only comparable to those achieved by single dose administration with particles.

In the case of the peptide-based vaccine (Figure 6A) a similar pattern of responses was observed although the reproducibility of the antibody response between animals receiving vaccine administered with particles was more variable than that observed when the protein-based vaccine was used. The variation in responses observed when peptide-based vaccine was used does not appear to be related to particle size because the mean difference in the range of antibody levels induced by each particle type was similar ($\log_{2.208}$ vs $\log_{2.362}$). Very little antibody was elicited by the peptide-based vaccine when administered in saline only.

Taken together, the results suggest that the use of chitosan-based nanoparticles or microparticles may be useful as a vaccine delivery system to enhance the immunogenicities of otherwise poorly immunogenic molecules or species.

DISCUSSION

Among the many current vaccine technologies available, the utilization of polymeric, biodegradable particle-based systems as vaccine delivery vehicles offers several advantages over other conventional vaccine approaches. Unlike live or attenuated vaccines, the possibility of virulence due to reversion and reassortment does not exist. Synthetic particle-based preparations also lend themselves to robust characterization and definition, and the methods of preparation employed in their manufacture allow for rational design and the introduction of various chemistries that can be used to tailor their composition. Chitosan is an ideal biopolymer for such purposes due to its nontoxic nature, biocompatibility and biodegradability and the ability to modify its physical and chemical properties to obtain the desired and appropriate features.

We have shown in this study that the use of chitosan nano- and microparticles can enhance the immunogenicity of otherwise nonimmunogenic peptide and protein antigens. Robust antibody responses against the self-hormone LHRH could be induced by inoculation of animals with two doses of antigen-conjugated particles, and in the case when protein was used as antigen, the level of antibody titers elicited was similar

dx.doi.org/10.1021/mp200264m | Mol. Pharmaceutics 2012, 9, 81–90

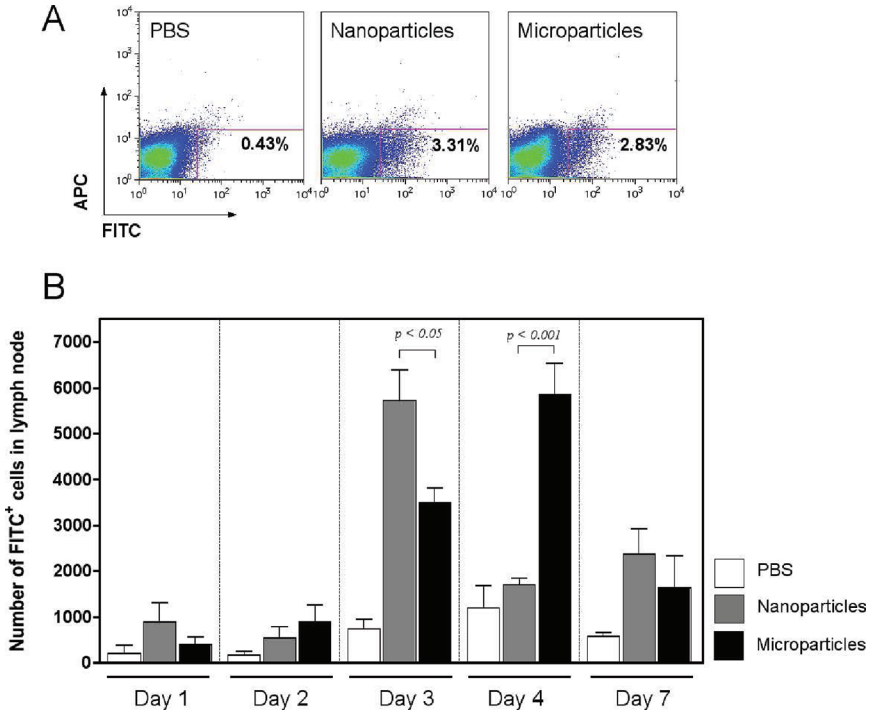

Figure 5. *In vivo* trafficking of fluoresceinated nanoparticles and fluoresceinated microparticles. BALB/c mice (8−10 weeks old) were inoculated in the hind footpad with 200 μg of fluorescently labeled microparticles (black bars) or fluorescently labeled nanoparticles (gray bars) in saline or were inoculated with PBS alone (clear bar). All inocula were administered in 50 μL volumes. Two mice from each group were killed at each of the time points examined and their popliteal lymph nodes (2 from each mouse) removed to obtain single cell suspensions that were then analyzed by flow cytometry. (A) The numbers of fluorescent cells in each sample were determined by visualizing fluorescence dot plots on the FL1 vs FL4 channels to eliminate cell-associated autofluorescence. The figures within each quadrant represent the average percentage of fluoresceinated cells in each sample. (B) Numbers of fluorescent cells associated with each lymph node (n = 4 per group).

to that induced when the antigen was administered with complete Freund's adjuvant, a very efficient but toxic adjuvant.

Nano- and microparticles manufactured by varying the surfactant HLB ratio in the emulsion-based assembly process were functionalized with chloroacetyl groups so that thiol-containing antigens could be covalently attached in a simple overnight incubation step under slightly basic conditions. The advantage of this approach is its relatively low cost in comparison to other methods such as the use of heterobifunctional linkers; the method also minimizes the possibility of antigen denaturing and degradation that can be associated with other antigen encapsulation processes.

The strategy of delivering antigen covalently attached to particles has previously proven to be better at inducing immune responses than has the coadministration of noncovalently attached antigen−particle systems.[2,3] Improved immunogenicity in the case of covalently attached antigen is perhaps not surprising and may be attributed to the *simultaneous* delivery of both antigen and particles to DCs. Such covalent associations are beneficial for uptake and colocalization to the same DC can lead to its activation,[35] antigen cross-presentation[36,37] and activation of naive T cells.[38] Furthermore the availability of multiple copies of antigens on the surface of particles could also be advantageous for B cell recognition and activation[39] resulting in more efficient antibody production.

Although the mechanisms associated with the induction of efficient immune responses mediated by chitosan-based particles are yet to be elucidated, it has been suggested that the immunostimulating properties of nanoparticles and microparticles may be related to their similarity in size to viruses and bacteria respectively and that the immune system has evolved to react to particles that fall within this size range.[15] Several studies have also pointed out that differences in particle size can have a significant effect on their interaction with APCs and the subsequent immune response[16−19] while others have noted no dissimilarities.[20,22] We have found in this study that although chitosan-based nano- and microparticles are taken up with comparable efficiency by DCs, they appear to traffic at different rates to draining lymph nodes with nanoparticles traveling to draining lymph nodes faster than microparticles. The findings of Manolova et al.[17] suggest that polystyrene nanoparticles drain directly into the lymphatics from the injection site and are taken up by resident lymph node cells while the trafficking of microparticles from the injection site is predominantly cell-mediated. While this finding could explain the more rapid appearance of nanoparticles in the lymph nodes in our experiments, the faster transit time of nanoparticles did not, however, impact immunogenicity because both nano- and microparticles exhibited similar ability in inducing antigen-specific antibody responses. These results also suggest an adjuvanting effect of the chitosan particles themselves possibly due to their behavior as charged polyelectrolytes. It is perhaps interesting to note the hydrophilicity of the chitosan particles used in this study compared to the hydrophobic nature of particles used in other studies. It may well be that the apparent differences in immunogenic properties previously attributed to particle size and reported in many studies is in fact associated with other physicochemical properties of the various materials used, the antigen type and route of vaccination.

Immunological approaches to controlling reproduction by modulating hormones such as LHRH represent a noninvasive and often effective form of endocrine therapy. LHRH is

dx.doi.org/10.1021/mp200264m | *Mol. Pharmaceutics* 2012, 9, 81−90

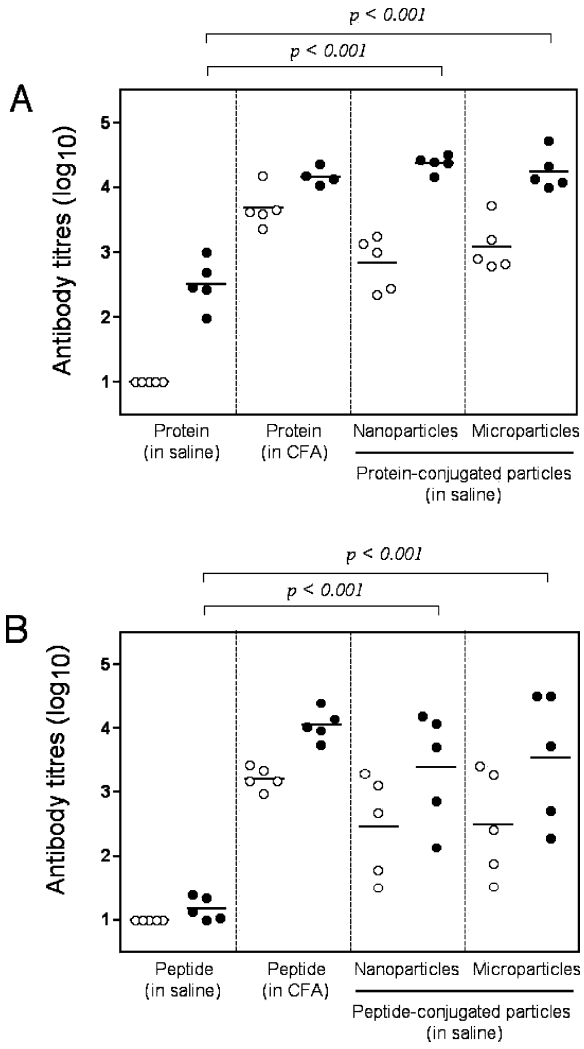

Figure 6. Immunogenicity of antigen-loaded nanoparticles and microparticles. Groups of BALB/c mice (n = 5 per group) were inoculated subcutaneously at the base of the tail with microparticles or nanoparticles containing 25 μg of protein (A) or 20 nmol of peptide antigen (B) in a volume of 100 μL. Mice were also inoculated with each antigen in saline only or antigen emulsified in CFA. Sera was obtained from blood taken 27 days after the primary (○) and 13 days following the secondary (●) inoculation. Antibody levels were then determined by ELISA. Individual animal titers are presented with the mean value represented by the horizontal bar within each graph.

secreted by the hypothalamus and is accessible to antibody-mediated intervention because it is transported in blood to the pituitary gland. Antibodies directed against this hormone therefore lead to the inhibition of reproductive capabilities of vaccinated animals, a facility of great benefit to the livestock industry in, for example, the elimination of boar taint[40] and also in companion animal husbandry by providing an alternative to surgical castration. While currently available LHRH-based vaccines require the coadministration of an adjuvant to induce effective responses, we have shown in this study that vaccination with chitosan-based nano- and microparticles that are loaded with LHRH-based peptide or protein antigens in the absence of adjuvant can elicit high titers of LHRH-specific antibodies at levels which have been previously associated with the inhibition of reproductive function.[24,41,42] More recently, the use of LHRH-based vaccines for reducing testosterone levels for the control of hormone-dependent malignancies in humans has also resulted in promising clinical outcomes.[27,29] Given the biocompatibility of chitosan and its apparent adjuvanting effects as well as its amenity to chemical and physical modifications, the approach to vaccine design that we have described here could represent another useful method for inducing immune responses against microbial, viral and tumorigenic protein antigens.

AUTHOR INFORMATION

Corresponding Author

*The University of Melbourne, Department of Microbiology and Immunology, Parkville, Victoria, Australia 3010. Tel: +61 3 8344-9940. Fax: +61 3 8344-9941. E-mail: d.jackson@microbiology.unimelb.edu.au.

ACKNOWLEDGMENTS

This work was supported by the Cooperative Research Centre for Polymers and the National Health & Medical Research Council of Australia. The authors would like to thank Dr. John Walker (Pfizer Inc., Parkville, Victoria, Australia) for provision of the protein-conjugate vaccine.

REFERENCES

(1) Arca, H. C.; Gunbeyaz, M.; Senel, S. Chitosan-based systems for the delivery of vaccine antigens. *Expert Rev. Vaccines* **2009**, *8*, 937–953.

(2) Slutter, B.; Bal, S. M.; Que, I.; Kaijzel, E.; Lowik, C.; Bouwstra, J.; Jiskoot, W. Antigen-adjuvant nanoconjugates for nasal vaccination: an improvement over the use of nanoparticles? *Mol. Pharmaceutics* **2010**, *7*, 2207–2215.

(3) Slutter, B.; Soema, P. C.; Ding, Z.; Verheul, R.; Hennink, W.; Jiskoot, W. Conjugation of ovalbumin to trimethyl chitosan improves immunogenicity of the antigen. *J. Controlled Release* **2010**, *143*, 207–214.

(4) Zaharoff, D. A.; Rogers, C. J.; Hance, K. W.; Schlom, J.; Greiner, J. W. Chitosan solution enhances both humoral and cell-mediated immune responses to subcutaneous vaccination. *Vaccine* **2007**, *25*, 2085–2094.

(5) Khatri, K.; Goyal, A. K.; Gupta, P. N.; Mishra, N.; Vyas, S. P. Plasmid DNA loaded chitosan nanoparticles for nasal mucosal immunization against hepatitis B. *Int. J. Pharm.* **2008**, *354*, 235–241.

(6) Zhou, X.; Zhang, X.; Yu, X.; Zha, X.; Fu, Q.; Liu, B.; Wang, X.; Chen, Y.; Shan, Y.; Jin, Y.; Wu, Y.; Liu, J.; Kong, W.; Shen, J. The effect of conjugation to gold nanoparticles on the ability of low molecular weight chitosan to transfer DNA vaccine. *Biomaterials* **2008**, *29*, 111–117.

(7) Amidi, M.; Romeijn, S. G.; Verhoef, J. C.; Junginger, H. E.; Bungener, L.; Huckriede, A.; Crommelin, D. J.; Jiskoot, W. N-trimethyl chitosan (TMC) nanoparticles loaded with influenza subunit antigen for intranasal vaccination: biological properties and immunogenicity in a mouse model. *Vaccine* **2007**, *25*, 144–153.

(8) Prego, C.; Paolicelli, P.; Diaz, B.; Vicente, S.; Sanchez, A.; Gonzalez-Fernandez, A.; Alonso, M. J. Chitosan-based nanoparticles for improving immunization against hepatitis B infection. *Vaccine 28*, 2607-2614.

(9) Sui, Z.; Chen, Q.; Fang, F.; Zheng, M.; Chen, Z. Cross-protection against influenza virus infection by intranasal administration of M1-based vaccine with chitosan as an adjuvant. *Vaccine* **2010**, *28*, 7690–7698.

(10) Amidi, M.; Pellikaan, H. C.; Hirschberg, H.; de Boer, A. H.; Crommelin, D. J.; Hennink, W. E.; Kersten, G.; Jiskoot, W. Diphtheria toxoid-containing microparticulate powder formulations for pulmonary vaccination: preparation, characterization and evaluation in guinea pigs. *Vaccine* **2007**, *25*, 6818–6829.

(11) Kang, M. L.; Kang, S. G.; Jiang, H. L.; Shin, S. W.; Lee, D. Y.; Ahn, J. M.; Rayamahji, N.; Park, I. K.; Shin, S. J.; Cho, C. S.; Yoo, H. S.

In vivo induction of mucosal immune responses by intranasal administration of chitosan microspheres containing Bordetella bronchiseptica DNT. *Eur. J. Pharm. Biopharm.* **2006**, *63*, 215−220.
(12) Sayin, B.; Somavarapu, S.; Li, X. W.; Thanou, M.; Sesardic, D.; Alpar, H. O.; Senel, S. Mono-N-carboxymethyl chitosan (MCC) and N-trimethyl chitosan (TMC) nanoparticles for non-invasive vaccine delivery. *Int. J. Pharm.* **2008**, *363*, 139−148.
(13) Florindo, H. F.; Pandit, S.; Goncalves, L. M.; Videira, M.; Alpar, O.; Almeida, A. J. Antibody and cytokine-associated immune responses to S. equi antigens entrapped in PLA nanospheres. *Biomaterials* **2009**, *30*, 5161−5169.
(14) Xie, Y.; Zhou, N. J.; Gong, Y. F.; Zhou, X. J.; Chen, J.; Hu, S. J.; Lu, N. H.; Hou, X. H. Th immune response induced by H pylori vaccine with chitosan as adjuvant and its relation to immune protection. *World J. Gastroenterol.* **2007**, *13*, 1547−1553.
(15) Fifis, T.; Gamvrellis, A.; Crimeen-Irwin, B.; Pietersz, G. A.; Li, J.; Mottram, P. L.; McKenzie, I. F.; Plebanski, M. Size-dependent immunogenicity: therapeutic and protective properties of nano-vaccines against tumors. *J. Immunol.* **2004**, *173*, 3148−3154.
(16) Mottram, P. L.; Leong, D.; Crimeen-Irwin, B.; Gloster, S.; Xiang, S. D.; Meanger, J.; Ghildyal, R.; Vardaxis, N.; Plebanski, M. Type 1 and 2 immunity following vaccination is influenced by nanoparticle size: formulation of a model vaccine for respiratory syncytial virus. *Mol. Pharmaceutics* **2007**, *4*, 73−84.
(17) Manolova, V.; Flace, A.; Bauer, M.; Schwarz, K.; Saudan, P.; Bachmann, M. F. Nanoparticles target distinct dendritic cell populations according to their size. *Eur. J. Immunol.* **2008**, *38*, 1404−1413.
(18) Reddy, S. T.; Rehor, A.; Schmoekel, H. G.; Hubbell, J. A.; Swartz, M. A. In vivo targeting of dendritic cells in lymph nodes with poly(propylene sulfide) nanoparticles. *J. Controlled Release* **2006**, *112*, 26−34.
(19) Chen, H. C.; Sun, B.; Tran, K. K.; Shen, H. Effects of particle size on toll-like receptor 9-mediated cytokine profiles. *Biomaterials* **2011**, *32*, 1731−1737.
(20) Cohen, J. A.; Beaudette, T. T.; Tseng, W. W.; Bachelder, E. M.; Mende, I.; Engleman, E. G.; Frechet, J. M. T-cell activation by antigen-loaded pH-sensitive hydrogel particles in vivo: the effect of particle size. *Bioconjugate Chem.* **2009**, *20*, 111−119.
(21) Tran, K. K.; Shen, H. The role of phagosomal pH on the size-dependent efficiency of cross-presentation by dendritic cells. *Biomaterials* **2009**, *30*, 1356−1362.
(22) Waters, K. M.; Masiello, L. M.; Zangar, R. C.; Tarasevich, B. J.; Karin, N. J.; Quesenberry, R. D.; Bandyopadhyay, S.; Teeguarden, J. G.; Pounds, J. G.; Thrall, B. D. Macrophage responses to silica nanoparticles are highly conserved across particle sizes. *Toxicol. Sci.* **2009**, *107*, 553−569.
(23) Delves, P. J.; Lund, T.; Roitt, I. M. Antifertility vaccines. *Trends Immunol.* **2002**, *23*, 213−219.
(24) Chua, B. Y.; Zeng, W.; Lau, Y. F.; Jackson, D. C. Comparison of lipopeptide-based immunocontraceptive vaccines containing different lipid groups. *Vaccine* **2007**, *25*, 92−101.
(25) Jung, M. J.; Moon, Y. C.; Cho, I. H.; Yeh, J. Y.; Kim, S. E.; Chang, W. S.; Park, S. Y.; Song, C. S.; Kim, H. Y.; Park, K. K.; McOrist, S.; Choi, I. S.; Lee, J. B. Induction of castration by immunization of male dogs with recombinant gonadotropin-releasing hormone (GnRH)-canine distemper virus (CDV) T helper cell epitope p35. *J. Vet. Sci.* **2005**, *6*, 21−24.
(26) Khan, M. A.; Ferro, V. A.; Koyama, S.; Kinugasa, Y.; Song, M.; Ogita, K.; Tsutsui, T.; Murata, Y.; Kimura, T. Immunisation of male mice with a plasmid DNA vaccine encoding gonadotrophin releasing hormone (GnRH-I) and T-helper epitopes suppresses fertility in vivo. *Vaccine* **2007**, *25*, 3544−3553.
(27) Talwar, G. P.; Vyas, H. K.; Purswani, S.; Gupta, J. C. Gonadotropin-releasing hormone/human chorionic gonadotropin beta based recombinant antibodies and vaccines. *J. Reprod. Immunol.* **2009**, *83*, 158−163.
(28) Oonk, H. B.; Turkstra, J. A.; Schaaper, W. M.; Erkens, J. H.; Schuitemaker-de Weerd, M. H.; van Nes, A.; Verheijden, J. H.; Meloen, R. H. New GnRH-like peptide construct to optimize efficient immunocastration of male pigs by immunoneutralization of GnRH. *Vaccine* **1998**, *16*, 1074−1082.
(29) Gonzalez, G.; Lage, A. Cancer vaccines for hormone/growth factor immune deprivation: a feasible approach for cancer treatment. *Curr. Cancer Drug Targets* **2007**, *7*, 229−241.
(30) Jackson, D. C.; Drummer, H. E.; Brown, L. E. Conserved determinants for CD4+ T cells within the light chain of the H3 hemagglutinin molecule of influenza virus. *Virology* **1994**, *198*, 613−623.
(31) Jackson, D. C.; Fitzmaurice, C. J.; Brown, L. E.; Zeng, W. Preparation and properties of totally synthetic immunogens. *Vaccine* **1999**, *18*, 355−361.
(32) Chua, B. Y.; Eriksson, E. M.; Poole, D. P.; Zeng, W.; Jackson, D. C. Dendritic cell acquisition of epitope cargo mediated by simple cationic peptide structures. *Peptides* **2008**, *29*, 881−890.
(33) Kato, K.; Utani, A.; Suzuki, N.; Mochizuki, M.; Yamada, M.; Nishi, N.; Matsuura, H.; Shinkai, H.; Nomizu, M. Identification of neurite outgrowth promoting sites on the laminin alpha 3 chain G domain. *Biochemistry* **2002**, *41*, 10747−10753.
(34) Ghosh, S.; Jackson, D. C. Antigenic and immunogenic properties of totally synthetic peptide-based anti-fertility vaccines. *Int. Immunol.* **1999**, *11*, 1103−1110.
(35) Shirota, H.; Sano, K.; Hirasawa, N.; Terui, T.; Ohuchi, K.; Hattori, T.; Shirato, K.; Tamura, G. Novel roles of CpG oligodeoxynucleotides as a leader for the sampling and presentation of CpG-tagged antigen by dendritic cells. *J. Immunol.* **2001**, *167*, 66−74.
(36) Heit, A.; Maurer, T.; Hochrein, H.; Bauer, S.; Huster, K. M.; Busch, D. H.; Wagner, H. Cutting edge: Toll-like receptor 9 expression is not required for CpG DNA-aided cross-presentation of DNA-conjugated antigens but essential for cross-priming of CD8 T cells. *J. Immunol.* **2003**, *170*, 2802−2805.
(37) Prajeeth, C. K.; Jirmo, A. C.; Krishnaswamy, J. K.; Ebensen, T.; Guzman, C. A.; Weiss, S.; Constabel, H.; Schmidt, R. E.; Behrens, G. M. The synthetic TLR2 agonist BPPcysMPEG leads to efficient cross-priming against co-administered and linked antigens. *Eur. J. Immunol.* **2010**, *40* (5), 1272−1283.
(38) Blander, J. M.; Medzhitov, R. Toll-dependent selection of microbial antigens for presentation by dendritic cells. *Nature* **2006**, *440*, 808−812.
(39) Fehr, T.; Skrastina, D.; Pumpens, P.; Zinkernagel, R. M. T cell-independent type I antibody response against B cell epitopes expressed repetitively on recombinant virus particles. *Proc. Natl. Acad. Sci. U.S.A.* **1998**, *95*, 9477−9481.
(40) Scaramuzzi, R. J.; Campbell, B. K.; Martin, G. B. Immunological approaches to fertility regulation in domestic livestock. *Immunol. Cell Biol.* **1993**, *71* (Part 5), 489−499.
(41) Zeng, W.; Gauci, S.; Ghosh, S.; Walker, J.; Jackson, D. C. Characterisation of the antibody response to a totally synthetic immunocontraceptive peptide vaccine based on LHRH. *Vaccine* **2005**, *23*, 4427−4435.
(42) Zeng, W.; Ghosh, S.; Lau, Y. F.; Brown, L. E.; Jackson, D. C. Highly immunogenic and totally synthetic lipopeptides as self-adjuvanting immunocontraceptive vaccines. *J. Immunol.* **2002**, *169*, 4905−4912.